Ionization of carbon, nitrogen, and oxygen by electron impact

Yong-Ki Kim
National Institute of Standards and Technology, Gaithersburg, Maryland 20899-8422

Jean-Paul Desclaux
15 Chemin du Billery, F-38360 Sassenage, France

(Received 22 February 2002; published 19 July 2002)

Total ionization cross sections of neutral carbon, nitrogen, and oxygen atoms by electron impact are presented. In our theory we have included the possibilities that (a) some target atoms used in an experiment were in metastable states close to the ground state, (b) excitation-autoionization of $2s2p^m$ exited states may be substantial, and (c) ions produced in experiments may be in excited, low-lying metastable states. The binary-encounter Bethe (BEB) model of Kim and Rudd [Phys. Rev. A **50**, 3954 (1994)] is used to calculate the cross sections for direct ionization. Plane-wave Born cross sections scaled by the method developed by Kim [Phys. Rev. **64**, 032713 (2001)] are used to determine the contributions from excitation-autoionization. A sum of the BEB cross sections for direct ionization weighted according to the statistical weights of the final ion states is used to modify the direct ionization cross sections. The combination of the BEB model and the scaled Born cross sections is in excellent agreement with available experimental data. The present method can easily be extended to heavier open-shell atoms.

DOI: 10.1103/PhysRevA.66.012708 PACS number(s): 34.80.Dp

I. INTRODUCTION

During the past decade, several powerful theoretical methods to calculate electron-impact ionization cross sections for the hydrogen atom have emerged in the literature [1–5]. These methods essentially solve the Schrödinger equation for two electrons with both electrons in the continuum, and are in principle capable of deducing differential ionization cross sections as well as total ionization cross sections. The detailed, sometimes overwhelming, volume of collision data from these theoretical methods requires substantial computational resources, and many of the methods are limited to one-electron atoms and atoms that can be represented by an effective one-electron model. Extensions of these methods [6,7] and extensions of the *R*-matrix method [8] to many-electron atoms are now appearing in the literature.

We anticipate that these fundamental theories will eventually provide collision data for atoms with complex structure with the steady progress in computing power. Until such time, however, there is an acute need for simple, flexible, and reliable theoretical methods to calculate electron-impact total ionization cross sections for the large number of neutral atoms and ions with open-shell structures that are used in a wide range of scientific and industrial applications, such as in astrophysics, atmospheric science, x-ray lasers, magnetic fusion, radiation physics, and semiconductor fabrication. For such applications, ionization cross sections must be reliable not only at high incident energies, but also at low and intermediate incident energies.

In this article theoretical total ionization cross sections, which were calculated using a combination of the binary-encounter Bethe (BEB) model [9] for direct ionization and scaled plane-wave Born (PWB) cross sections for excitation-autoionization [10], are compared to available experimental data on carbon, nitrogen, and oxygen. For these and most open-shell atoms in the periodic table, several issues unique to open-shell atoms must be addressed to obtain reliable total ionization cross sections.

The first issue is the initial state of the target atom. Because most open-shell atoms have metastable terms close to the ground term with the same electronic configuration, a substantial number of target atoms may be in such metastable terms depending on the way the target atoms are prepared in an experiment. For example, Brook *et al.* [11] and Freund *et al.* [12] generated target atoms by neutralizing positive ions through charge exchange. Their experimental data on the threshold behavior clearly demonstrate that some of their target atoms such as nitrogen, phosphorus, and arsenic were in metastable terms.

The second issue is the indirect ionization through excitation-autoionization. For aluminum, for instance, the autoionization of the $3s3p^2\,{}^2S$ and ${}^2P$ terms contributes to the total ionization almost as much as the direct ionization of the $3s$ and $3p$ electrons [13] does. The fact that some atoms may initially be in a metastable term brings another level of complication; the important autoionizing states are different for the ground and metastable terms because the spin quantum numbers for the ground and metastable terms are usually different.

The third issue is that in most experiments no distinction is made of the final state of the ions produced. Most open-shell atoms will produce ions that also have metastable terms with the same electronic configuration as the ground term of the ion. This problem is solved in a rigorous theory by choosing the appropriate exit channels. However, the BEB model [9] does not explicitly use final-state wave functions. Within the context of the BEB model, exit channels can be identified only by using different ionization energies needed to reach metastable ion states from the initial state of a target

atom. A simple way that is compatible with the BEB model to calculate partial cross sections for the production of different ion states is presented in this paper.

The main objective of this paper is to demonstrate that the combination of the BEB model [9] and scaled Born cross sections for dominant inner-shell excitation-autoionization [10] produces total ionization cross sections of modest accuracy ($\sim$15% or better at the cross section peak) that are reliable from the threshold to several keV in the incident electron energy with far less computational effort than any existing method. This combination can easily be extended to more complex open-shell atoms to obtain ionization cross sections of similar accuracy, using the cases presented in this paper as examples for homologous atoms in the same columns of the periodic table.

Theoretical methods are outlined in Sec. II, applications of the methods to individual atoms and comparisons to available theoretical and experimental results are presented in Sec. III, and conclusions are drawn in Sec. IV.

II. OUTLINE OF THEORY

A. BEB cross section for individual ion states

The binary-encounter Bethe model [9] is a simplified version of the binary-encounter dipole (BED) model. The BED model combines the Mott cross section [14] with the leading dipole part of the Bethe cross section [15,16], and provides singly differential (in secondary electron energy) ionization cross sections by electron impact. The total ionization cross section is then obtained by integrating the differential cross section over the secondary electron energy.

In contrast, the BEB model provides only the total ionization cross section for each orbital in the target atom or molecule using the orbital binding energy B, the orbital kinetic energy $U=\langle p^2/2m\rangle$, and the orbital electron occupation number N. Neither the BED model nor the BEB model contains any adjustable or empirical parameters.

The BEB cross section for direct ionization of an electron in a bound orbital by an electron of incident energy T is given by [9]

$$\sigma_{\mathrm{BEB}}=\frac{4\pi a_0^2 N(B/R)^2}{t+u+1}\left[\frac{\ln t}{2}\left(1-\frac{1}{t^2}\right)+1-\frac{1}{t}-\frac{\ln t}{1+t}\right], \qquad (1)$$

where a_0 is the Bohr radius, R is the Rydberg energy, $t=T/B$, and $u=U/B$. On the right-hand side of Eq. (1), the first logarithmic term came from the leading part of the Bethe cross section, the middle term $1-1/t$ from the direct and pure exchange part of the Mott cross section, and the last logarithmic term from the interference between the direct and exchange terms of the Mott cross section. The denominator $t+u+1$ is often used in binary-encounter theory [17] to emulate the effective incident energy as seen by the target bound electron. The denominator reduces cross sections near the threshold, where many first-order perturbation theories such as the plane-wave and distorted-wave Born approximations overestimate cross sections.

B. BEB cross section for plural ion states

Note that the target data used in σ_{BEB}, i.e., B, U, and N, are those for the initial state only. No final-state data are used explicitly, except indirectly through the ionization energy B. This simplicity based on orbitals serves as an advantage for the BEB model when it is applied to complex atoms [18] and molecules [19,20].

However, the lack of explicit information on final-state channels in the BEB model makes it necessary to modify the model when the resulting ions have more than one LS term, where L and S are the total orbital and spin angular momenta. For instance, when the nitrogen atom is ionized, the electronic configuration of N^+ is $2p^2$, which produces three LS terms, ^3P, ^1D, and ^1S. (The J-dependent fine structure, where J is the total angular momentum, becomes important only for heavy atoms and highly charged ions.) Most experiments on total ionization cross sections do not distinguish the resulting ion states, and hence the theory must sum over these final states, which are often metastable. Ionization energies from the ground levels of C, N, and O and ionization energies from the metastable levels of N are listed in Table I.

The ratios of the ions in different final states that belong to the same electronic configuration of the ion are expected to approach the statistical ratios [i.e., the ratios of $2J+1$ or $(2L+1)(2S+1)$] in the limit of high T as the coupling between the different final-state channels diminishes and eventually disappears. Near the threshold, resonances dominate the region between the thresholds for different ion states. The BEB model is too simple to reproduce such resonances. To preserve the simplicity of the BEB model and at the same time be consistent with the expected asymptotic (high T) ratios of the partial cross sections to produce different ion states, we multiply the BEB cross sections for individual final ion states by the expected statistical ratios, i.e., weight them according to the statistical ratios, before we sum them to obtain the total ionization cross section.

The weighted BEB cross sections are given by

$$\sigma_{LS}=\frac{(2L+1)(2S+1)}{\sum_{L'S'}(2L'+1)(2S'+1)}\sigma_{\mathrm{BEB}LS}, \qquad (2)$$

where $\sigma_{\mathrm{BEB}LS}$ is the BEB cross section to produce an ion in a given LS term calculated from Eq. (1) using the appropriate ionization energies (Table I). The sum over L' and S' covers all final ion states with quantum numbers $L'S'$ that share the same electron configuration. Of course, L and S are one of the allowed L''s and S''s. The cross section σ_{LS} is the weighted or partial cross section for the ions in the LS term among all ions produced.

The total ionization cross section is then given by

$$\sigma_{ion}=\sum_{LS}\sigma_{LS}. \qquad (3)$$

For instance, in the above example of N^+ (1) three different σ_{BEB}'s for the three ion terms ^3P, ^1D, and ^1S, are calculated using appropriate ionization energies B; (2) the cross

TABLE I. Ionization energies of C, N, and O in eV [25].

Atom	Level	Ion	Level	Ionization energy
C	$2s^2 2p^2\ ^3P_{0,1}$	C^+	$2s^2 2p\ ^2P_{1/2}$	11.26
			$2s^2 2p\ ^2P_{3/2}$	11.27
	$2s^2 2p^2\ ^3P_2$		$2s^2 2p\ ^2P_{1/2}$	11.25
			$2s^2 2p\ ^2P_{3/2}$	11.26
N	$2s^2 2p^3\ ^4S_{3/2}$	N^+	$2s^2 2p^2\ ^3P_0$	14.53
			$2s^2 2p^2\ ^3P_1$	14.54
			$2s^2 2p^2\ ^3P_2$	14.55
			$2s^2 2p^2\ ^1D_2$	16.43
			$2s^2 2p^2\ ^1S_0$	18.59
	$2s^2 2p^3\ ^2D_{5/2,3/2}$		$2s^2 2p^2\ ^3P_{0,1}$	12.15
			$2s^2 2p^2\ ^3P_2$	12.17
			$2s^2 2p^2\ ^1D_2$	14.05
			$2s^2 2p^2\ ^1S_0$	16.20
	$2s^2 2p^3\ ^2P_{3/2,1/2}$		$2s^2 2p^2\ ^3P_{0,1}$	10.96
			$2s^2 2p^2\ ^3P_2$	10.97
			$2s^2 2p^2\ ^1D_2$	12.86
			$2s^2 2p^2\ ^1S_0$	15.01
O	$2s^2 2p^4\ ^3P_2$	O^+	$2s^2 2p^3\ ^4S_{3/2}$	13.62
			$2s^2 2p^3\ ^2D_{5/2,3/2}$	16.94
			$2s^2 2p^3\ ^2P_{3/2,1/2}$	18.64
	$2s^2 2p^4\ ^3P_1$		$2s^2 2p^3\ ^4S_{3/2}$	13.60
			$2s^2 2p^3\ ^2D_{5/2}$	16.92
			$2s^2 2p^3\ ^2D_{3/2}$	16.93
			$2s^2 2p^3\ ^2P_{3/2,1/2}$	18.62
	$2s^2 2p^4\ ^3P_0$		$2s^2 2p^3\ ^4S_{3/2}$	13.59
			$2s^2 2p^3\ ^2D_{5/2}$	16.91
			$2s^2 2p^3\ ^2D_{3/2}$	16.92
			$2s^2 2p^3\ ^2P_{3/2,1/2}$	18.61

sections are weighted by 9/15, 5/15, and 1/15, respectively, for the three ion states; and then (3) the weighted cross sections are summed to obtain the total ionization cross section. These weighted cross sections may not be realistic partial cross sections for the production of metastable ions close to their thresholds where resonances dominate. However, the comparisons to available experiments shown in the next section indicate that the overall behavior of the total ionization cross sections obtained through Eq. (3) agrees well with experiments in most of the incident energy range.

C. Excitation-autoionization

The BEB cross section describes only direct ionization, i.e., direct ionization of a bound electron resulting from the collision of the primary and secondary electrons. For open-shell atoms, there are often additional, indirect channels of ionization, such as the excitation of an inner-shell electron to an upper bound state that leads to autoionization. When the outermost orbital of an atom is not fully occupied, electrons in the core orbitals can be excited to the outermost orbital. Excitations of this kind may produce excited states which lie either below or above the first ionization limit. The excited states above the first ionization limit must decay either by photoemission without producing an ion or by autoionization by ejecting an electron. When the core electron comes from an orbital with the same principal quantum number as the outermost orbital (e.g., $2s2p^m$), cross sections of such excitation-autoionizations tend to be large, sometimes matching the magnitude of direct ionization cross section [13]. Cross sections for these indirect channels must be calculated separately and added to the BEB cross sections for direct ionization before BEB cross sections can be compared to experimental results.

There are excitations of the $2s$ electrons to higher "bound" levels, such as $2s2p^3\ ns$, np, nd, $n \geqslant 3$, that will autoionize. However, we found such higher excitations contribute $\sim 5\%$ or less in Al [13]. We expect these higher excitations to contribute less in C, N, and O because the smaller ratios of the occupation number of the $2s$ and $2p$ electrons in the latter will make the autoionization of the $2s$ excited levels less significant compared to the direct ionization of the $2p$ electrons. In addition, there are many other effects that we have neglected that will change the total ionization cross section by a few percent, such as the interference between these autoionizing levels and the background continuum. For these reasons, we have included only the autoionization of levels from the $2s \rightarrow 2p$ excitations.

Again, to preserve the simplicity of the BEB model, we look for a simple way to estimate the contributions from dominant excitation-autoionization channels, keeping in mind that our goal is to calculate total ionization cross sections with a modest accuracy. With this goal, we only have to account for the autoionization of states that can be reached from the initial state of the target atom by dipole- and spin-allowed transitions.

The scaled PWB cross section for electron-impact excitation described in [10], to be referred to as the BE scaling hereafter, has been developed to address this need:

$$\sigma_{\mathrm{BE}} = \frac{T}{T+B+E}\,\sigma_{\mathrm{PWB}}, \tag{4}$$

where E is the excitation energy and σ_{PWB} is the PWB cross section for dipole- and spin-allowed excitations.

When σ_{PWB} is calculated from inaccurate target wave functions it must be scaled further by the ratio of the accurate dipole oscillator strength f_{accu} to the f value calculated from the same wave functions used to calculate the PWB excitation cross section f_{PWB}. This is referred to as f scaling [10]:

$$\sigma_f = \frac{f_{\mathrm{accu}}}{f_{\mathrm{PWB}}}\,\sigma_{\mathrm{PWB}}. \tag{5}$$

Note that the f scaling given by Eq. (5) is different from past efforts to modify (or create) electron-impact cross sections using f values, e.g., the Gaunt-factor method. Unlike past efforts, the f scaling multiplies the ratio of f values to the entire σ_{PWB} without changing its shape. The shape of σ_{PWB} is altered by the BE scaling. In other words, the BE scaling corrects the shortcomings of the Born approximation, while

the f scaling corrects the errors introduced by inaccurate wave functions. These two scalings can be used consecutively, if appropriate. As has been demonstrated for atoms ranging from hydrogen to thallium [10], the BE scaling and f scaling transform PWB cross sections into results comparable to convergent-close-coupling cross sections [1] and accurate experiments.

III. RESULTS AND DISCUSSION

Most of the theoretical work on the ionization of C, N, and O published in the 1980s and earlier are variations of the first-order Born approximations, such as the plane-wave, Coulomb-wave, and distorted-wave Born approximations, for both direct ionization and excitation-autoionization and with or without electron exchange. These methods based on the first-order Born approximation produce cross sections too high at low and intermediate T, and the variations used were mostly to reduce cross sections at low T. Such theories had limited success as can be seen in comparisons to experiments summarized by Brook *et al.* [11] for C, N, and O, and by Chung *et al.* [21] for O.

Experimental data available by the late 1970s are summarized by Brook *et al.* [11]. For oxygen, additional experimental data have been reported by Zipf [22] and by Thompson *et al.* [23] after the experiment by Brook *et al.* In this section, we will compare our theoretical results to the experimental data for C and N by Brook *et al.*, and the data for O by Brook *et al.*, Zipf, and Thompson *et al.* As was mentioned earlier, Brook *et al.* prepared target neutral atoms by neutralizing positive ions by charge exchange. This preparation sometimes produces significant amount of metastable atoms. On the other hand, Zipf and Thompson *et al.* used dissociation of O_2 to avoid the production of metastable O in any significant amount.

Our theory also contains elements of the first-order Born approximation such as the Bethe cross section in Eq. (1) and σ_{PWB} in Eqs. (4) and (5), while the Mott cross section in Eq. (1) is an all-order theory, albeit for an idealized collision of two free electrons. However, our final result emulates all-order theory by replacing the incident energy $t=T/B$ by $t+u+1=(T+U+B)/B$ in Eq. (1) and T by $T+B+E$ in Eq. (4). This simple shifting of T by a constant amount related to the target structure effectively emulates most of the higher order interactions between the incident and target electrons, such as electron exchange, distortion of the incident wave, and the polarization of the target charge distribution, viz., the correlation between the two colliding electrons [9,10,24].

The magnitudes of the excitation cross sections that contribute to excitation-autoionization depend on the LSJ quantum numbers of the upper and lower levels. We included only (electric) dipole- and spin-allowed excitations so that we could apply the BE scaling described in Sec. II C.

The ground terms of neutral carbon ($2s^2 2p^2\ ^3P$) and neutral oxygen ($2s^2 2p^4\ ^3P$) have fine structures, while the ground term of neutral nitrogen ($2s^2 2p^3\ ^4S$) has no fine structure. Carbon, nitrogen, and oxygen have metastable terms with the same electronic configurations as their ground terms but with different total spin and total orbital angular momenta. The existence of metastable target atoms can often be confirmed in experiments by significant ionization below the correct ionization threshold for the ground term, because metastable terms have lower ionization energies. This is the case for the experimental data on nitrogen by Brook *et al.* [11] as will be shown later.

To take advantage of our existing computing capability for atomic wave functions, f values, and PWB cross sections, we have used Dirac-Fock wave functions to generate necessary theoretical data (B, U, N, PWB excitation cross sections, f values, etc.), although relativistic effects are insignificant in C, N, and O. To match the experimental thresholds, we used experimental ionization and excitation energies for metastable and autoionizing states obtained from the public website of the National Institute of Standards and Technology (NIST) [25].

For clarity, we use the shorthand notations $2p_{1/2} \equiv 2p_-$ and $2p_{3/2} \equiv 2p_+$ for the relativistic orbitals, and $2p$ for the nonrelativistic orbital. For BEB cross sections for direct ionization, appropriate J^2 eigenstates are built from only $2s$, $2p_+$, and $2p_-$ orbitals. For PWB cross sections for excitation-autoionization, multiconfiguration Dirac-Fock (MCDF) wave functions were built from orbitals with the principal quantum number $n=2$ and 3. Only doubly excited configurations were used for correlation orbitals, and all orbitals were made self-consistent. Proper overlap integrals were included in transition matrix elements to account for the fact that the orbitals in the initial and final states were not orthogonal.

We used the orbital energies as the binding energies B, except that the B value for the least bound orbital was replaced by the experimental ionization energy. Orbital occupation numbers N for the $2s$, $2p_-$, and $2p_+$ orbitals have been calculated from the mixing coefficients of relativistic configurations for individual J^2 eigenfunctions. The resulting values of B, U, and N are listed in Table II, along with excitation energies and f values for the autoionizing levels.

The total widths of the fine-structure splitting in the ground states of C and O are small (0.0054 eV for C and 0.028 eV for O), and hence we have assumed that the target atoms are distributed among the fine-structure levels according to their statistical weights, i.e., $2J+1$. Excitation cross sections to the autoionizing levels depend on the initial-state and final-state J values, and hence the total excitation cross sections must be averaged over the initial-state J values.

On the other hand, the fine-structure splittings in individual ion terms are small, resulting in almost identical B values for the ion levels with different J but the same L and S, and consequently almost identical direct ionization cross sections. Therefore, we simply used the B values for the lowest fine-structure level within a given LS term of an ion, and assumed that the direct ionization cross sections for the different J levels of a given ion term are the same.

Although the use of relativistic wave functions results in extra computations compared to nonrelativistic wave functions, relativistic treatment is nevertheless needed when we apply our theoretical method to heavy atoms such as iodine whose fine-structure splitting in the ground term is almost 1 eV.

A. Carbon

The ground configuration of C^+ is $2s^2 2p\,^2P$, and there is no metastable term with the same configuration. The fine-structure splitting in the ground term of C^+ is ~ 0.008 eV, and as was explained earlier we calculated separate cross sections for the different J levels only in the ground term of C.

The direct ionization cross section for each of the three J levels in the ground term of C was calculated using Eq. (1), weighted by $(2J+1)/9$, and summed to get the total direct ionization cross section. Note that in Table II the orbital occupation numbers N for the $2p_-$ and $2p_+$ orbitals for C are strongly dependent on J while the U values are almost independent of J.

Since the ground term of C is a triplet, the only autoionizing triplet term with the configuration $2s2p^3$ which is located above the ionization limit is the ^3S term at 13.117 eV above the ground level of C [25]. The electric dipole selection rule allows each of the three J levels of the ground term of C to be excited to the autoionizing level $2s2p^3\,^3S_1$. Multiconfiguration Dirac-Fock wave functions constructed from $n=2$ and 3 orbitals were used for both the ground and excited terms of C to calculate the PWB excitation cross sections. Then, the PWB excitation cross sections were scaled using Eq. (4) and added to the direct ionization cross sections for each J to obtain the total ionization cross section of C with a specific J. Finally, these J-specific ionization cross sections were averaged with the weight of $2J+1$ to get the total ionization cross section of C.

Adding an excitation cross section to a matching direct ionization cross section to obtain the total ionization cross section implies an assumption that the branching ratio for autoionization of the excited state of C is practically 100%, as is common for light atoms. At present, we do not have any reliable data on the branching ratio between the decay by photoemission and autoionization. (This situation is different for oxygen as is discussed in Sec. III C.)

The direct, autoionizing, and total ionization cross sections are listed in Table III. Although the listed cross sections have been averaged over the initial-state fine structure because we have used relativistic wave functions, individual J-dependent cross sections are very close, within a few percent at the peak, as expected from weak relativistic effects in carbon. Our total ionization cross section agrees well with the experimental data by Brook *et al.* [11] as shown in Fig. 1. The experimental data do not show significant cross section at the ionization threshold, indicating that the target beam did not contain many metastable atoms. The theoretical cross sections in Fig. 1 also do not include cross sections for metastable carbon atoms.

Wiese *et al.* [26] list f values for the $2s^2 2p^2\,^3P - 2s2p^3\,^3S$ transitions. These values came from the Opacity Project, in which nonrelativistic wave functions were used. The single nonrelativistic multiplet f value from the Opacity Project was split into line values for J-J' pairs using the relative intensities within an LS multiplet [27]. The f values listed by Wiese *et al.* [26] for this transition are about a factor of 2 smaller than the f values we have obtained from MCDF wave functions. If we were to adopt the f values from the Opacity Project, then we could apply the f scaling [Eq. (5)] using the ratio of the f values from Wiese *et al.* and our f values from the MCDF wave functions. The use of the f values from Wiese *et al.* would reduce the contributions of excitation-autoionization by about one-half.

Under normal circumstances, the f values from an R-matrix calculation with a large number of bound states are expected to be more accurate than the f values calculated from MCDF wave functions of limited size. However, since the f value from the Opacity Project relevant to the present case was calculated using the R-matrix method with pseudo-orbitals to emulate continuum states, it is unclear if f values from the R-matrix method for states above the first ionization limit are as reliable as the f values for bound states close to the ground state. We chose to trust our MCDF f values instead. Our results in Table III and Fig. 1 are without f scaling and indicate that about 20% of the total ionization cross section comes from excitation-autoionization.

B. Nitrogen

The ground term of N is $2s^2 2p^3\,^4S$, and there are no quartet $2s2p^4$ states above the first ionization limit. Hence, if the target atoms belonged solely to the $^4S_{3/2}$ level, there would be no significant contribution to the total ionization cross section from excitation-autoionization.

However, the experimental data by Brook *et al.* [11] shown in Fig. 2 clearly exhibit a small but discernible cross section at $T \leqslant 14$ eV, indicating the presence of metastable target atoms. The relevant metastable terms are $2s^2 2p^3\,^2D$ and ^2P, which are 2.38 eV and 3.58 eV above the ground level, respectively. Atoms in these metastable terms can be excited to autoionizing $2s2p^4$ doublet states, if they exist. There should be a ^4P, and ^2P, ^2D, and ^2S terms from the $2s2p^4$ configuration. According to the energy levels compiled by NIST [25], the ^4P term is in the discrete spectrum, and only the ^2D term is observed at 15.03 eV above the ground level.

In an article by Ericsson [28], who reported the observation of the emission line emanating from the $2s2p^4\,^2D_{5/2}$ level, he stated: ''Owing to the large perturbations between the series $(2s^2 2p^2)\ ns\,^2P_{3/2}$, $nd\,^2P_{3/2}$, and $nd\,^4F_{3/2}$ only a rough extrapolation was carried out. . . .'' This kind of perturbation can easily cause the $2s2p^4\,^2P$ term to be ''scattered'' among the perturbing series. Ericsson identified the $2s2p^4\,^2D_{5/2}$ level through the 4107.9 Å line to the $2s^2 2p^2 3p\,^2D_{5/2}$ level. Our MCDF calculations with a limited number of configurations indicate that the ^2S and ^2P terms should be within a few eV of the ^2D term, if they existed. The usual selection rules are favorable for transitions from the ^2S and ^2P terms to terms with the same $2s^2 2p^2 3p$ configuration, making such lines easily detectable by Ericsson's experiment.

Moreover, Hibbert *et al.* [29] reported an extensive table of f values for nitrogen based on large-scale configuration mixing. They reported transitions from the $2s2p^4\,^2D$ term, but nothing from the $2s2p^4\,^2S$ and ^2P terms. For the ^2D

TABLE II. Atomic parameters for the BEB and scaled Born cross sections. *B*, binding energy; *U*, orbital kinetic energy; *N*, electron occupation number; *E*, excitation energy; f_{mc}, *f* values calculated from MCDF wave functions; $f_{WFD}=f$ values from Wiese *et al*. [26]. Energy values marked by an asterisk are experimental.

Orbital	*B* (eV)	*U* (eV)	*N*	Initial level	Autoionizing level	*E* (eV)	f_{mc}	f_{WFD}
				Carbon, ground (^3P)				
$1s_{1/2}$	308.304	437.156	2	$2s^22p^2\,^3P_0$	$2s2p^3\,^3S_1$	13.117*	0.2697	0.152
$2s_{1/2}$	19.213	41.911	2					
$2p_{1/2}$	11.786	34.121	1.3361					
$2p_{3/2}$	11.260*	34.107	0.6639					
$1s_{1/2}$	308.307	437.156	2	$2s^22p^2\,^3P_1$	$2s2p^3\,^3S_1$	13.115*	0.2705	0.152
$2s_{1/2}$	19.214	41.912	2					
$2p_{1/2}$	11.793	34.132	1					
$2p_{3/2}$	11.258*	34.091	1					
$1s_{1/2}$	308.312	437.158	2	$2s^22p^2\,^3P_2$	$2s2p^3\,^3S_1$	13.112*	0.2705	0.152
$2s_{1/2}$	19.216	41.915	2					
$2p_{1/2}$	11.787	34.125	0.3350					
$2p_{3/2}$	11.255*	34.098	1.6650					
				Nitrogen, ground (^4S)				
$1s_{1/2}$	425.469	598.726	2	$2s^22p^3\,^4S_{3/2}$				
$2s_{1/2}$	25.828	65.656	2					
$2p_{1/2}$	15.439	51.094	1.0025					
$2p_{3/2}$	14.534*	51.034	1.9975					
				Nitrogen, metastable (^2D)				
$1s_{1/2}$	426.561	603.371	2	$2s^22p^3\,^2D_{5/2}$	$2s2p^4\,^2D_{5/2}$	12.643*	0.2618	0.0481
$2s_{1/2}$	26.253	61.732	2		$2s2p^4\,^2D_{3/2}$	12.643*	0.0195	0.0034
$2p_{1/2}$	12.151*	49.207	1					
$2p_{3/2}$	14.013	49.833	2					
$1s_{1/2}$	426.483	598.752	2	$2s^22p^3\,^2D_{3/2}$	$2s2p^4\,^2D_{5/2}$	12.642*	0.0280	0.00496
$2s_{1/2}$	26.330	66.350	2		$2s2p^4\,^2D_{3/2}$	12.642*	0.2531	0.0468
$2p_{1/2}$	14.314	50.187	1					
$2p_{3/2}$	12.150*	49.340	2					
				Nitrogen, metastable (^2P)				
$1s_{1/2}$	426.780	607.488	2	$2s^22p^3\,^2P_{3/2}$	$2s2p^4\,^2D_{5/2}$	11.451*	0.1282	0.0331
$2s_{1/2}$	27.417	58.286	2		$2s2p^4\,^2D_{3/2}$	11.451*	0.0141	0.0035
$2p_{1/2}$	10.959*	48.655	1					
$2p_{3/2}$	13.462	49.277	2					
$1s_{1/2}$	426.780	607.475	2	$2s^22p^3\,^2P_{1/2}$	$2s2p^4\,^2D_{3/2}$	11.451*	0.1426	0.0364
$2s_{1/2}$	27.403	58.273	2					
$2p_{1/2}$	14.348	50.466	1					
$2p_{3/2}$	10.959*	48.423	2					
				Oxygen, ground (^3P)				
$1s_{1/2}$	562.878	796.189	2	$2s^22p^4\,^3P_2$	$2s2p^5\,^3P_2$	15.655*	0.2552	0.0465
$2s_{1/2}$	33.913	84.762	2		$2s2p^5\,^3P_1$	15.664*	0.0856	0.0155
$2p_{1/2}$	16.603	68.505	1.6748					
$2p_{3/2}$	13.618*	69.652	2.3252					
$1s_{1/2}$	562.895	796.194	2	$2s^22p^4\,^3P_1$	$2s2p^5\,^3P_2$	15.635*	0.1422	0.0258
$2s_{1/2}$	33.918	84.771	2		$2s2p^5\,^3P_1$	15.645*	0.0850	0.0155
$2p_{1/2}$	18.271	70.600	1		$2s2p^5\,^3P_0$	15.650*	0.1139	0.0207
$2p_{3/2}$	13.598*	68.674	3					
$1s_{1/2}$	562.818	790.474	2	$2s^22p^4\,^3P_0$	$2s2p^5\,^3P_1$	15.636*	0.3385	0.0619
$2s_{1/2}$	34.010	90.499	2.0000					
$2p_{1/2}$	19.810	71.730	0.6649					
$2p_{3/2}$	13.590*	68.636	3.3351					

TABLE III. Cross sections of the carbon atom in Å^2 for direct ionization, for excitations to the $2s2p^3\,{}^3S_1$ autoionizing level, and for the total ionization as functions of the incident electron energy T in eV.

T	Direct	Excitation $2s^22p^2\,{}^3P-2s2p^3\,{}^3S$	Total
12	0.0526		0.0526
14	0.243	0.120	0.362
16	0.423	0.202	0.625
18	0.582	0.248	0.831
20	0.737	0.279	1.016
25	1.116	0.323	1.439
30	1.391	0.345	1.736
35	1.587	0.354	1.942
40	1.726	0.358	2.084
45	1.823	0.357	2.180
50	1.890	0.354	2.244
60	1.963	0.344	2.307
70	1.985	0.332	2.317
80	1.978	0.319	2.297
90	1.954	0.307	2.261
100	1.920	0.295	2.215
120	1.838	0.273	2.111
150	1.708	0.245	1.953
180	1.586	0.222	1.807
200	1.511	0.209	1.720
250	1.349	0.183	1.532
300	1.218	0.163	1.380
350	1.110	0.147	1.257
400	1.021	0.134	1.155
450	0.945	0.124	1.069
500	0.881	0.115	0.995
600	0.776	0.100	0.876
700	0.695	0.0896	0.784
800	0.630	0.0810	0.711
900	0.577	0.0740	0.651
1000	0.532	0.0683	0.601
2000	0.308	0.0394	0.347
3000	0.220	0.0283	0.248
4000	0.173	0.0223	0.195
5000	0.143	0.0185	0.161

term, they added a footnote: ''. . . the corresponding eigenvector does not have unambiguously dominant component.''

Therefore, we conclude that the $2s2p^4\,{}^2S$ and ^2P terms have lost their distinct identities through mixing either with the $2s^22p^2ns$ and nd ^2S and ^2P series or with the underlying continuum background. Confirmation of the missing ^2P and ^2S terms through heavy configuration mixing requires elaborate calculations, which are beyond the scope of the present work. We included only the excitations to the ^2D term from the two metastable terms of N.

The ground term of N^+ is $2s^22p^2\,{}^3P$, and the ion has two metastable terms, $2s^22p^2\,{}^1D$ and ^1S at 1.90 eV and 4.05 eV above the ground level of N^+, respectively [25]. To calculate

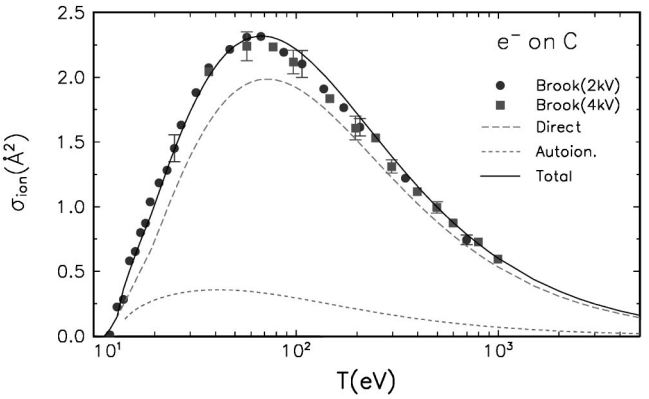

FIG. 1. Ionization cross sections of the carbon atom as functions of the incident electron energy T. The circles and squares are experimental total ionization cross sections by Brook *et al.* [11] using 2 keV and 4 keV ion beams, respectively; the medium-dashed curve is the direct ionization cross section based on the BEB model; the short-dashed curve is the BE-scaled Born cross section for the $2s^22p^2\,{}^3P-2s2p^3\,{}^3S$ excitation; and the solid curve is the total ionization cross section.

the partial cross sections for direct ionization, we used Eq. (1) with the U and N values from the MCDF wave functions of the ground and metastable states of N, and the ionization energies B needed to reach the three ion terms ^3P, ^1D, or ^1S (see Table I). The form of Eq. (1) makes the cross section larger if the B of the outermost electron is lower. Hence the direct ionization cross section for producing N^+ in the ^3P term is the highest. In addition, the statistical weight $(2L+1)(2S+1)$ of 9 for the ^3P term is the largest, followed by 5 and 1 for the ^1D and ^1S terms, respectively. The combination of the lowest B value and the largest weight makes the

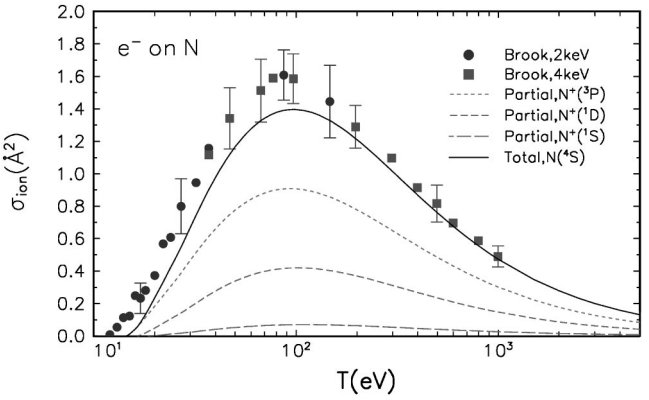

FIG. 2. Partial cross sections of the nitrogen atom as functions of the incident electron energy T. The circles and squares are experimental total ionization cross section by Brook *et al.* [11] using 2 keV and 4 keV ion beams, respectively; the short-dashed curve is the partial cross section for producing the ground-state ion $N^+(^3P)$; the medium-dashed curve is the partial cross section for producing the metastable ion $N^+(^1D)$; the long-dashed curve is the partial cross section for producing the metastable ion $N^+(^1S)$; and the solid curve is the sum of the partial cross sections, i.e., the total ionization cross section of the ground-state atom $N(^4S)$.

TABLE IV. Cross sections of the nitrogen atom in Å^2 for the direct ionization, for excitation-autoionization, and for total ionization from the ground level $2s^2 2p^3\ ^4S$ and metastable ^2D and ^2P terms, and the cross section for the ground (70%)–metastable (30% ^2D) mixture as functions of the incident electron energy T in eV.

T	From ^4S	From ^2D			From ^2P			70-30 Mix
	Total	Direct	Excitation	Total	Direct	Excitation	Total	
12					0.00335	0.120	0.123	
14		0.0499	0.224	0.274	0.0263	0.273	0.300	0.0822
16	0.0415	0.167	0.325	0.492	0.0706	0.411	0.481	0.177
18	0.132	0.303	0.381	0.684	0.121	0.540	0.661	0.298
20	0.235	0.433	0.417	0.849	0.169	0.653	0.822	0.419
25	0.464	0.703	0.463	1.166	0.268	0.870	1.137	0.675
30	0.669	0.925	0.481	1.406	0.344	1.026	1.370	0.890
35	0.843	1.110	0.485	1.594	0.408	1.151	1.559	1.068
40	0.979	1.251	0.482	1.733	0.458	1.243	1.700	1.205
45	1.084	1.359	0.475	1.834	0.495	1.309	1.804	1.309
50	1.166	1.441	0.467	1.907	0.523	1.356	1.879	1.389
60	1.278	1.548	0.446	1.995	0.560	1.411	1.971	1.493
70	1.343	1.606	0.426	2.031	0.578	1.432	2.010	1.550
80	1.378	1.632	0.405	2.037	0.587	1.432	2.019	1.576
90	1.394	1.638	0.387	2.025	0.588	1.421	2.008	1.583
100	1.396	1.631	0.369	2.001	0.584	1.401	1.985	1.577
120	1.377	1.596	0.338	1.934	0.570	1.351	1.921	1.544
150	1.321	1.517	0.300	1.817	0.540	1.266	1.806	1.470
180	1.255	1.432	0.270	1.702	0.509	1.183	1.692	1.389
200	1.210	1.377	0.254	1.630	0.489	1.132	1.620	1.336
250	1.105	1.250	0.220	1.470	0.443	1.018	1.461	1.215
300	1.014	1.142	0.195	1.337	0.404	0.925	1.328	1.111
350	0.935	1.051	0.175	1.226	0.371	0.846	1.218	1.022
400	0.868	0.972	0.159	1.132	0.343	0.781	1.124	0.947
450	0.810	0.905	0.146	1.052	0.319	0.725	1.044	0.882
500	0.759	0.848	0.136	0.983	0.299	0.677	0.976	0.826
600	0.675	0.752	0.118	0.871	0.265	0.599	0.864	0.734
700	0.609	0.677	0.105	0.783	0.238	0.538	0.776	0.661
800	0.555	0.617	0.095	0.712	0.217	0.489	0.705	0.602
900	0.510	0.566	0.087	0.653	0.199	0.448	0.647	0.553
1000	0.473	0.524	0.080	0.604	0.184	0.415	0.599	0.512
2000	0.278	0.307	0.046	0.352	0.107	0.241	0.348	0.300
3000	0.200	0.220	0.0325	0.253	0.0771	0.173	0.250	0.216
4000	0.158	0.173	0.0256	0.199	0.0606	0.136	0.197	0.170
5000	0.131	0.144	0.0212	0.165	0.0502	0.113	0.163	0.141

partial cross section for the production of N^+ (^3P) the largest (from direct ionization). The weighted partial cross sections for producing different ion terms from the ground term of N and the sum of the partial cross sections is shown in Fig. 2. The total ionization cross section from the ground term of N alone, however, is visibly lower than the experimental data, as can be seen in Fig. 2.

For metastable target N atoms, we must also include excitation-autoionization involving the $2s2p^4\ ^2D$ term in the continuum because both metastable terms ^2D and ^2P can reach the excited term by dipole- and spin-allowed transitions. Since the fine-structure splittings in the doublet terms of metastable N are very small, we assumed statistical population of the target atoms in the fine-structure levels, and averaged excitation cross sections accordingly. We used MCDF wave functions to calculate PWB excitation cross sections and transformed them by BE scaling, Eq. (4). In this manner, we can generate total ionization cross sections as if all target atoms are in one of the three terms, the ground and two metastable. The direct, autoionizing, and total ionization cross sections from the ground level ^4S and ^2D and ^2P metastable terms are tabulated in Table IV. We have assumed 100% branching ratio for autoionization from the $2s2p^4\ ^2D$ excited term, as we did for carbon.

A surprising result is that the cross sections for the ^2D and ^2P metastable terms of N are almost identical, except very near the thresholds, which are separated by about 1.2 eV (see Fig. 3). This makes our task of guessing the fraction of metastable atoms present in the target beam used by Brook *et al.* [11] easy. We found that a mixture of 70% ground level and 30% metastable ^2D term matches the experimental cross section very well, as can be seen in Fig. 3. If it turned out that the *missing* autoionizing terms ($2s2p^4\,^2S$ and ^2P) actually existed above the lowest ionization threshold, then excitation cross sections and hence autoionization contributions from each metastable target atom would be higher than the excitation to the $2s2p^3\,^2D$ term we have included, and consequently the fraction of metastable atoms would be reduced.

Table II also lists *f* values for the excitations of metastable N (^2D and ^2P) tabulated by Wiese *et al.* [26]. These *f* values are about a factor of 5 smaller than our values calculated from MCDF wave functions. The values tabulated by Wiese *et al.* were calculated by Hibbert *et al.* [29] using nonrelativistic wave functions with correlation and intermediate coupling. As was the case for carbon, the objective of Hibbert *et al.* was to obtain the best *f* values for the transitions between bound levels below the lowest ionization limit. The use of the *f* values by Hibbert *et al.* with Eq. (5) would drastically reduce the excitation-autoionization cross sections listed in Table IV, and hence make the total ionization cross section shown in Fig. 3 lower than the experimental data by Brook *et al.* [11], particularly near the threshold.

C. Oxygen

As was mentioned earlier, Zipf [22] and Thompson *et al.* [23] produced oxygen atoms by dissociating O_2 to avoid the production of metastable oxygen, unlike the experiment by Brook *et al.* [11]. The comparison of the three sets of experimental data, however, suggests that the oxygen beam used by Brook *et al.* did not contain large fractions of metastables.

We calculated cross sections only for the ground term of O, $2s^22p^4\,^3P$. The O^+ ion has two metastable terms, $2s^22p^3\,^2D$ and ^2P. The only autoionizing term that can be reached from the ground term (^3P) by dipole- and spin-allowed excitation is the $2s2p^5\,^3P$ term. In Fig. 4, we compare experimental data by Zipf [22] and by Thompson *et al.* [23] for both single ionization to the partial cross sections for producing O^+ ions in three different terms and the direct ionization cross section from the ground term of O (^3P).

The $2s2p^5\,^3P$ term is located at about 15.66 eV above the ground level. Excitation cross sections to the autoionizing term were calculated using MCDF wave functions, then scaled by Eq. (4). The values of *B*, *U*, *N*, excitation energies *E*, and *f* values are listed in Table II, and the direct, autoionizing, and total ionization cross sections are listed in Table V.

The population of the ground-state *J* levels was averaged by statistical weight, the population of the ion levels among the ground and metastable terms was weighted also according to their statistical weight, and only those excitations between the ground term of O to the autoionizing term which were allowed by the selection rule for the dipole- and spin-allowed transitions were included in the autoionization contribution.

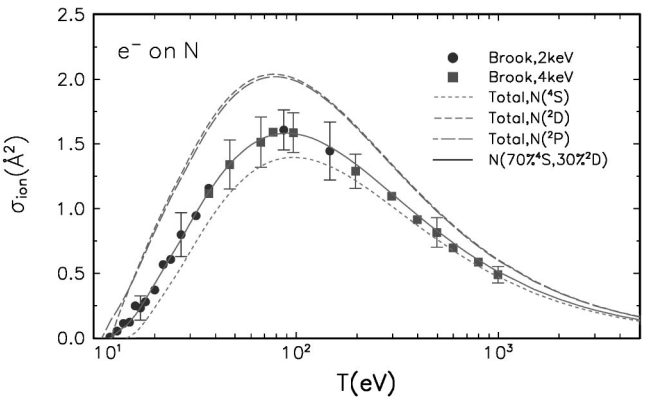

FIG. 3. Ionization cross sections of the nitrogen atom as functions of the incident electron energy *T*. The circles and squares are experimental total ionization cross sections by Brook *et al.* [11] using 2 keV and 4 keV ion beams, respectively; the short-dashed curve is the total ionization cross section of the ground state N(^4S); the medium-dashed curve is the total ionization cross section of the metastable N(^2D); the long-dashed curve is the total ionization cross section of the metastable N(^2P); and the solid curve is the total ionization cross section of a mixture (70% ^4S, 30% ^2D) of N in the ground and metastable states.

Unlike the case of carbon and nitrogen, Dehmer *et al.* [30] reported that the branching ratio for autoionization of the $2s2p^5\,^3P$ term is about 50% according to their photoionization experiment. From their experiment, we deduced branching ratios of 59.7% for the autoionization of the upper $J'=0$ level, 55.5% for the $J'=1$ level, and 47.2% for the $J'=2$ level. We applied these branching ratios to the excitation

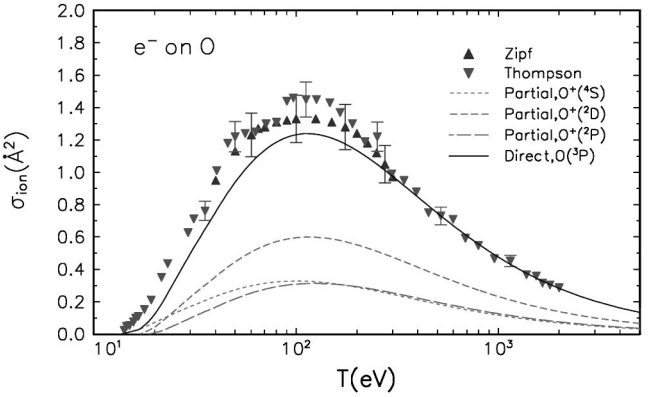

FIG. 4. Partial cross sections of the oxygen atom as functions of the incident electron energy *T*. The triangles are the experimental total ionization cross section by Zipf [22]; the inverted triangles are the total ionization cross section by Thompson *et al.* [23]; the short-dashed curve is the partial cross section for producing the ground-level ion $O^+(^4S)$; the medium-dashed curve is that for the metastable ion $O^+(^2D)$; the long-dashed curve is that for the metastable ion $O^+(^2P)$; and the solid curve is the direct ionization cross section of the ground-state atom O(^3P).

TABLE V. Cross sections of the oxygen atom in Å^2 for the direct ionization, excitation-autoionization, and total ionization from the ground term $2s^2 2p^4\ ^3P$ as functions of the incident electron energy T in eV.

T	Direct	Excitation $2s^2 2p^4\ ^3P - 2s2p^5\ ^3P$	Total
14	0.00383		0.00383
16	0.0247	0.0464	0.0711
18	0.0651	0.112	0.178
20	0.133	0.144	0.277
25	0.334	0.185	0.519
30	0.509	0.205	0.714
35	0.649	0.215	0.864
40	0.767	0.220	0.987
45	0.868	0.222	1.091
50	0.951	0.223	1.173
60	1.071	0.219	1.290
70	1.149	0.214	1.363
80	1.198	0.208	1.406
90	1.227	0.201	1.428
100	1.243	0.195	1.437
120	1.247	0.182	1.430
150	1.220	0.165	1.385
180	1.175	0.151	1.336
200	1.142	0.143	1.285
250	1.058	0.126	1.185
300	0.981	0.113	1.094
350	0.912	0.103	1.015
400	0.852	0.0939	0.946
450	0.799	0.0867	0.885
500	0.752	0.0806	0.832
600	0.673	0.0708	0.744
700	0.610	0.0633	0.673
800	0.558	0.0573	0.615
900	0.514	0.0524	0.567
1000	0.478	0.0483	0.526
2000	0.284	0.0279	0.312
3000	0.205	0.0201	0.225
4000	0.162	0.0158	0.178
5000	0.135	0.0131	0.148

cross sections before we added them to the direct ionization cross sections to obtain the total ionization cross section.

In Fig. 5, our total ionization cross section is compared to the experiments by Brook *et al*. [11], Zipf [22], and Thompson *et al*. [23] and to the theoretical results by Chung *et al*. [21], who calculated the direct ionization cross sections from the distorted-wave Born cross sections with the Ochkur approximation for electron exchange, and PWB cross sections without electron exchange. Again, we see excellent agreement of the present work with the experiments particularly at low T. Thompson *et al*. reported a small but distinct step at the peak near $T=100$ eV, which is not visible in the other two sets of experimental data. From the atomic structure data, we cannot find any process that could produce such a step near $T=100$ eV.

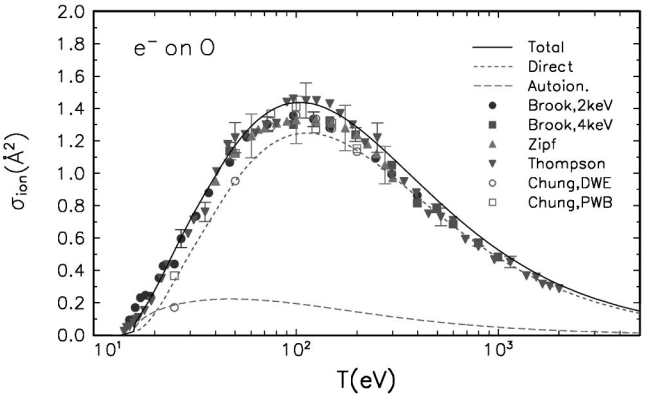

FIG. 5. Ionization cross sections of the oxygen atom as a function of the incident electron energy T. The solid curve is our total ionization cross section; short-dashed curve is that for direct ionization; medium-dashed curve is that for excitation-autoionization; filled circles and filled squares are experimental total ionization cross sections for single ionization by Brook *et al*. [11] with 2 keV and 4 keV target beams, respectively; triangles are those by Zipf [22]; inverted triangles are those by Thompson *et al*. [23]; open circles are the distorted-wave Born cross section with the Ochkur approximation for electron exchange by Chung *et al*. [21]; open squares are plane-wave Born cross sections without exchange by Chung *et al*. [21]. The theory of Chung *et al*. is for direct ionization only.

As is the case for carbon and nitrogen, the excitation-autoionization in oxygen increases the total ionization cross section by 15%–20% at the peak. It is clear, however, that major excitation-autoionization channels must be included to obtain good agreement between theory and experiment at low T.

As is the case for nitrogen, the f values for oxygen from the Opacity Project and tabulated by Wiese *et al*. [26] are about a factor of 5 smaller than our values calculated from MCDF wave functions (see Table II). Using the Opacity Project f values with Eq. (5) would reduce the excitation-autoionization cross sections listed in Table V, and hence reduce the total ionization cross section shown in Fig. 5, particularly near the threshold where the autoionization contributes more than the direct ionization.

IV. CONCLUSIONS

We have shown that a combination of the BEB theory [9] for the direct ionization and scaled Born cross sections for a few dominant excitation-autoionization channels produces total ionization cross sections of carbon, nitrogen, and oxygen in excellent agreement with available experimental data at all incident electron energies.

Cross sections for the production of metastable ions with the same electronic configuration as the ground state of the ion has been accounted for by weighting the BEB cross sections for the production of individual ion states according to the statistical weights of the ion states.

Only those $2s2p^m$ states which can be reached from the initial state of the neutral atoms by electric dipole- and spin-

allowed transitions have been included in the autoionization contribution. Plane-wave Born cross sections for such excitations were calculated from multiconfiguration relativistic wave functions constructed from $n=2$ and 3 orbitals. Then BE scaling [10] was applied to make them valid at low as well as high incident electron energies.

Comparisons to experiments indicate that (a) excitation-autoionization increases the peak cross sections by 15%–20%, (b) theoretical cross sections near the ionization thresholds become much closer to experimental cross sections when dominant excitation-autoionization channels are included, (c) the experimental data for carbon and oxygen by Brook *et al*. [11] agree well with the present theoretical cross sections based on the assumption that the target atoms were in the ground state, (d) and their data on nitrogen agree well with the theory if we assume that the target beam consisted of 70% ground state and 30% metastable atoms.

For carbon and nitrogen, we assumed that all $2s$ excited electrons decayed through autoionization, whereas for oxygen we used the branching ratio of $\sim 50\%$ in accordance with the photoionization study by Dehmer *et al*. [30]. We found unexpectedly that the cross sections for excitation-autoionization of the $2s^2 2p^3\, ^2D$ and ^2P metastable nitrogen are almost identical except close to their thresholds.

Unlike other experiments, that of Thompson *et al*. [23] reported a small step near the cross section peak at about 100 eV in the incident electron energy in their experimental cross section for oxygen. We did not find such a step in our theoretical cross section, nor did a close examination of oxygen structure data reveal any process that might be responsible for such a step.

The f values associated with the excitations to autoionizing states and tabulated by Wiese *et al*. [26] are smaller than the f values we have calculated from correlated relativistic wave functions by a factor of 2–5. The f values tabulated by Wiese *et al*., however, were calculated from wave functions optimized for transitions between bound states below the lowest ionization thresholds, and not for the autoionizing states above the ionization thresholds. The use of the smaller f values with Eq. (5) would reduce the excitation cross sections listed in Tables III–V, resulting in far smaller total ionization cross sections near the ionization thresholds in Figs. 1, 3, and 5.

The combination of theories described in the present work not only can easily be extended to heavier atoms, as has been demonstrated for aluminum, gallium, and indium [13], but also offers a simple physical picture of dominant processes contributing to the total ionization cross section. As a by-product, an estimate of the partial cross sections for producing metastable ions can be obtained from the weighted BEB cross sections described in Sec. II B. To calculate total ionization cross sections for singly charged ions, the BEB model modified for ions [31] can be used for direct ionization, while the BE-scaled PWB cross sections for excitation-autoionization are replaced by E-scaled Coulomb-Born cross sections described in [24].

ACKNOWLEDGMENTS

This work was supported in part by the Office of Fusion Energy Sciences, U.S. Department of Energy, and by the Advanced Technology Program, NIST. We thank Dr. P. Indelicato for his assistance in developing the relativistic wave function code we have used.

[1] D.V. Fursa and I. Bray, Phys. Rev. A **52**, 1279 (1995); J. Phys. B **30**, 5895 (1997), and references therein.
[2] D. Kato and S. Watanabe, Phys. Rev. Lett. **74**, 2443 (1995).
[3] M. Baertschy, T.N. Rescigno, and C.W. McCurdy, Phys. Rev. A **64**, 022707 (2001), and references therein.
[4] F. Robischeaux, M.S. Pindzola, and D.R. Plante, Phys. Rev. A **55**, 3573 (1997).
[5] S. Jones and D.H. Madison, Phys. Rev. A **62**, 042701 (2000), and references therein.
[6] D.V. Fursa, S. Trajmar, I. Bray, I. Kanik, G. Csanak, R.E.H. Clark, and J. Abdallah, Jr., Phys. Rev. A **60**, 4590 (1999).
[7] M.S. Pindzola, J. Colgan, F. Robicheaux, and D.C. Griffin, Phys. Rev. A **62**, 042705 (2000), and references therein.
[8] K. Bartschat, E. Hudson, P. Scott, P. Burke, and V. Burke, J. Phys. B **29**, 115 (1996); Phys. Rev. A **54**, R998 (1996), and references therein.
[9] Y.-K. Kim and M.E. Rudd, Phys. Rev. A **50**, 3954 (1994).
[10] Y.-K. Kim, Phys. Rev. A **64**, 032713 (2001).
[11] E. Brook, M.F.A. Harrison, and A.C.H. Smith, J. Phys. B **11**, 3115 (1978).
[12] R.S. Freund, R.C. Wetzel, R.J. Shul, and T.R. Hayes, Phys. Rev. A **41**, 3575 (1990), and references therein.
[13] Y.-K. Kim and P.M. Stone, Phys. Rev. A **64**, 052707 (2001).
[14] N.F. Mott, Proc. R. Soc. London, Ser. A **126**, 259 (1930).
[15] H. Bethe, Ann. Phys. (Leipzig) **5**, 325 (1930).
[16] M. Inokuti, Rev. Mod. Phys. **43**, 297 (1971).
[17] L. Vriens, in *Case Studies in Atomic Physics*, edited by E.W. McDaniel and M.R.C. McDowell (North-Holland, Amsterdam, 1969), Vol. 1, p. 335.
[18] Y.-K. Kim, J.P. Santos, and F. Parente, Phys. Rev. A **62**, 052710 (2000).
[19] H. Nishimura, W.M. Huo, M.A. Ali, and Y.-K. Kim, J. Chem. Phys. **110**, 3811 (1999), and references therein.
[20] NIST Electron-Impact Ionization Cross Section Database (Version 2.1), http://physics.nist.gov/ionxsec
[21] S. Chung, C.C. Lin, and E.T.P. Lee, Phys. Rev. A **47**, 3867 (1993).
[22] E.C. Zipf, Planet. Space Sci. **33**, 1303 (1985).
[23] W.R. Thompson, M.B. Shah, and H.B. Gilbody, J. Phys. B **28**, 1321 (1995).
[24] Y.-K. Kim, Phys. Rev. A **65**, 022705 (2002).
[25] NIST Atomic Spectra Database (Version 2.0), http://physics.nist.gov/asd
[26] W.L. Wiese, J.R. Fuhr, and T.M. Deters, J. Phys. Chem. Ref. Data Monogr. **7**, 522 (1996).
[27] See, for example, C. Cowley, W.L. Wiese, J. Fuhr, and L.A.

Kuznetsova, in *Allen's Astrophysical Quantities*, 4th ed., edited by A.N. Cox (Springer-Verlag, New York, 2000), Chap. 4, Sec. 4.5.
[28] K.B.S. Ericsson, Phys. Scr. **9**, 151 (1974).
[29] A. Hibbert, E. Biémont, M. Godefroid, and N. Vaeck, Astron. Astrophys., Suppl. Ser. **88**, 505 (1991).
[30] P.M. Dehmer, W.L. Luken, and W.A. Chupka, J. Chem. Phys. **67**, 195 (1977).
[31] Y.-K. Kim, K.K. Irikura, and M.A. Ali, J. Res. Natl. Inst. Stand. Technol. **105**, 285 (2000).